Dear Editor Eleanor Browne and Referee,

Thanks for your suggestions which significantly help us to improve the manuscript. Hereby, we submit our responses and the manuscript has been revised accordingly. If there are any further questions or comments, please let us know.

Best regards

Guoxian Zhang on behalf of all co-authors
Key Lab. of Environmental Optics & Technology, Anhui Institute of Optics and Fine Mechanics, Chinese Academy of Sciences
230031 Hefei China
E-mail: gxzhang@aiofm.ac.cn

Major Comments

1. ***Species X to match the observation. This is nothing more than a fitting exercise and does not really help us understanding what mechanism might be behind. Could be removed.***

Reply:

Thank you for your review and valuable comments on this manuscript. We agree with your perspective on Species X, considering its current role more as a fitting parameter, which may offer limited help in understanding the underlying mechanisms. However, in Section 3.3, we compared the oxidizing capacity of different urban agglomerations in China, using Species X as a comparative factor to demonstrate the extent of missing OH radical sources in various regions. Therefore, in this revision, we have decided to retain the discussion on Species X. Furthermore, to enhance the depth of the research and understanding of the mechanisms, we have incorporated the higher aldehyde mechanism (HAM) in subsequent studies and tested its impact on OH radicals, thereby complementing the discussion on Species X.

2. ***Introduction of more monoterpenes which might sustain a lower-than-expected HO2 to RO2 ratio due to the chemistry of complex alkoxy radicals. This in the current version of the paper is not well explained though. How does the RACM-LIM1 treats the alkoxy radicals formed from alpha-pinene and limonene? Did the author modified the mechanisms including available SAR? How is the organic nitrate yield treated? A recent study by Färber et al. (2024) shows that it might be difficult to sustain a lower than 0.6 HO2-to-RO2 ratio due to termination reaction for complex RO2 such as formation of organic nitrates. The section in the paper showing the sensitivity test including monoterpenes should give more information.***

Reply:

Thank you for your reply. The oxidation processes of α-pinene and limonene related to RACM2 mechanism have been listed in Table S4, including the oxidation reactions with $OH/O_3/NO_3$, as well as the reactions of the derived alkoxy radicals

(APIP) with $NO/NO_3/HO_2$ and the self-reactions among peroxy radicals. In the RACM2 mechanism, the peroxy radicals generated from α-pinene oxidation are classified as APIP and return to HO_2 radicals through subsequent reactions with NO. This manuscript has not modified the mechanisms including the available structure-activity relationships (SAR), and the yield of organic nitrates still uses the results from the RACM2-LIM1 mechanism, which is specifically described in Table S4. The sensitivity testing section that includes monoterpenes has provided more information on Lines 535-555.

We followed the reviewers' suggestions and added a discussion on the HO_2/RO_2 ratio in Section 4.2. Regarding the HO_2/RO_2 ratio issue for experiments and simulations, we have summarized the HO_2/RO_2 radical concentration ratios derived from radical concentrations measured by laser-induced fluorescence instruments and calculated using the MCM or RACM mechanisms in Fig. 10. If HO_2 is formed from an RO_2 radical, it would result in an HO_2/RO_2 radical concentration ratio of approximately 1. In field studies, the observed HO_2/RO_2 ratios were between 0.2 - 1.7 under low-NO conditions (NO < 1 ppb) and only 0.1 - 0.8 under high-NO conditions (3 < NO < 6 ppb). From the perspective of model-observation matching, except for three measurements in ClearfLo, ICOZA and AIRPRO-summer campaigns, the HO_2/RO_2 ratios in other regions could be reasonably reflected by the MCM or RACM2 mechanisms. However, the ratio is generally underestimated under high NO conditions, reaching up to 5 times in ClearfLo. According to the latest chamber experiments, the HO_2/RO_2 radical concentration ratios for VOCs forming HO_2 are 0.6 for both one-step and two-step reactions. Therefore, the extremely low HO_2/RO_2 ratios observed in field campaigns can only be explained if almost all RO_2 radicals undergo multiple-step reactions before forming HO_2. During the TROPSTECT campaign, the observed HO_2/RO_2 remains at 1.1 and 0.8 under low-NO and high-NO conditions, respectively. After considering the complex sources of complex alkoxy radicals in the 'MTS+X' scenario, the simulated values of HO_2/RO_2 in both low-NO and high-NO regions match the observed values well.

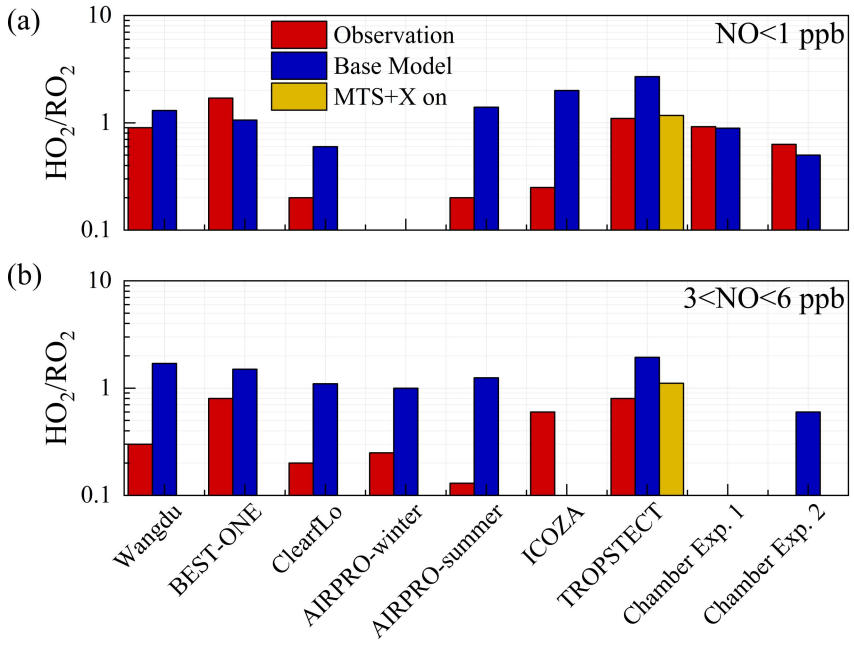

Fig. 10. Summary of the HO_2/RO_2 ratios derived from radical concentrations measured by laser-induced fluorescence instruments and calculated using the MCM or RACM models under **(a)** low-NO and **(b)** high-NO conditions. Charmber Exp. 1 and Charmber Exp. 2 denotes the parameters by single-step HO_2 formation and multi-step HO_2 formation determined in the chamber by (Färber et al., 2024).

Revision:

Line 535-555: An additional reaction was added to the base model in a previous research, converting OH into C96O2 (the oxidation product of α-pinene) with a reaction rate equal to the missing reactivity, to explore the source of the missing RO_2 radicals(Whalley et al., 2021). Discrepancy of OH reactivity (~3 – 5 s^{-1}) between measurement and model suggested that an additional driving force was necessary to complete the OH to RO_2 step. In the TROPSPECT campaign, approximately 0.4 ppb of monoterpene was introduced into the base scenario as the chemical reactions of complex alkoxy radicals, which is similar to an atmospheric level in the EXPLORE-2018 campaign, the YRD region (Wang et al., 2022a). The RACM2 mechanism identified α-pinene (API) and limonene (LIM) as representative monoterpenes species. Sensitivity tests were conducted by incorporating API and LIM into the 'MTS on' and 'MTS+X on' scenarios, respectively (Ma et al., 2022). The mean of these values was considered the average effect of monoterpenes chemistry, and depicted as the green line in Fig. 6. In the 'MTS on' scenario, the chemistry of peroxy radicals in Semi II was reasonably described by introducing the source of complex alkoxy radicals, and the obs-to-mod ratio of peroxy radicals decreased from 2.2 to 1.3.

Furthermore, the introduction of additional complex alkoxy radicals had minimal impact on HOx chemistry, with changes in daytime OH and HO_2 concentrations of less than 5×10^5 cm^{-3} and 2.5×10^7 cm^{-3}, respectively. This demonstrates the robustness of HOx radical in response to potential monoterpene.

Line 635-654: The HO_2/RO_2 parameter was utilized to explore the transformation relationship between HO_2 and RO_2 radicals. If HO_2 is formed from an RO_2 radical, it would result in an HO_2/RO_2 radical concentration ratio of approximately 1. The HO_2/RO_2 ratios derived from radical concentrations measured by laser-induced fluorescence instruments and calculated using the MCM or RACM models were summarized in Fig. 10. In field studies, the observed HO_2/RO_2 ratios were between 0.2 - 1.7 under low-NO conditions (NO < 1 ppb) and only 0.1 - 0.8 under high-NO conditions (3 < NO < 6 ppb). From the perspective of model-observation matching, except for three measurements in ClearfLo, ICOZA and AIRPRO-summer campaigns, the HO_2/RO_2 ratios in other regions could be reasonably reflected by the MCM or RACM2 mechanisms(Woodward-Massey et al., 2023; Whalley et al., 2021; Whalley et al., 2018; Färber et al., 2024). However, the ratio is generally underestimated under high NO conditions, reaching up to 5 times in ClearfLo. According to the latest chamber experiments, the HO_2/RO_2 radical concentration ratios for VOCs forming HO_2 are 0.6 for both one-step and two-step reactions. Therefore, the extremely low HO_2/RO_2 ratios observed in field campaigns can only be explained if almost all RO_2 radicals undergo multiple-step reactions before forming HO_2. During the TROPSTECT campaign, the observed HO_2/RO_2 remains at 1.1 and 0.8 under low-NO and high-NO conditions, respectively. After considering the complex sources of complex alkoxy radicals in the 'MTS+X' scenario, the simulated values of HO_2/RO_2 in both low-NO and high-NO regions match the observed values well.

3. ***The last "manipulation" of the mechanisms is not really clear to me. In the text it is mentioned: "Manipulating the self-reaction rate of peroxy radicals by approximately five-fold, and the extended lifetime counterbalance their supplementary consumption by non-traditional regeneration mechanisms"***

(Page 18 lines 465-467). I have no idea of what this means practically in the mechanism. This needs to be explained in a clearer way.

Reply:

Thank you for your reply. The last 'manipulation' of the mechanisms is based on the 'MTS+X' scenario, aiming to test the impact of reducing the rate coefficients between peroxy radicals on the concentration of RO_2 radicals. We acknowledge that this part of the content has little connection with other sensitivity tests, therefore we have deleted this discussion and supplemented the relevant discussion on the impact of the HAM mechanism on RO_2 radicals.

Table.1. The sensitive test scenarios utilized to improve the model-measurement consistency between OH, HO_2 and RO_2 radicals.

Scenario	Configuration	Purpose
Base	RACM2 updated with isoprene reaction scheme (LIM)	The base case with the species involved in Table S3 are constrained as boundary conditions.
X on	As the base scenario, but add the X mechanism, and the X level is between 0.25 - 0.5 ppb.	To untangle the missing OH source where base scenario failed.
MTS on	As the base scenario, but add a monoterpene source, and the monoterpene level is ~0.4 ppb.	Utilizing monoterpene-derived RO_2 to represent the alkoxy radicals with rather complex chemical structures.
MTS+X on	As the base scenario, but both the X mechanism and monoterpene source are considered.	To consider both the missing OH and RO_2 sources.
HAM on	As the base scenario, but add the reactive aldehyde chemistry.	To provide a test of whether the proposed mechanism can explain the missing OH source.
HAM on (4 × ALD)	As the base scenario, but add the reactive aldehyde chemistry, and the concentration of ALD was amplified by a factor of 4.	To quantify the impact of missing aldehyde primary emissions on ROx chemistry.
Ozone simulation	As the base scenario, but remove the constraints of the observed ozone and NO concentrations.	To test the suitable lifetime for the base model.
HCHO simulation	As the base scenario, but remove the constraint of the observed HCHO concentration.	To test the simulation effect of the existing mechanism on formaldehyde concentration.

Revision:

Line 556-569: Higher aldehyde chemistry is a concrete manifestation of verifying the aforementioned hypothesis for RO_2 sources(Yang et al., 2024b). The autoxidation process of $R(CO)O_2$, encompasses a hydrogen migration process that transforms it

into the ·OOR(CO)OOH radical(Wang et al., 2019). This radical subsequently reacts with NO to yield the ·OR(CO)OOH radical. The ·OR(CO)OOH radical predominantly undergoes two successive rapid hydrogen migration reactionss, ultimately resulting in the formation of HO_2 radicals and hydroperoxy carbonyl (HPC). Consequently, the HAM mechanism extends the lifetime of the RO_2 radical, providing a valuable complement to the unaccounted sources of RO_2 radicals. As depicted in Fig. 7, the incorporation of the HAM mechanism results in an approximate 7.4% and 12.5% increase in the concentrations of HO_2 and RO_2 radicals, respectively. It is important to note that the total concentrations of primary emitted aldehydes and the HPC group may be underestimated, which could lead to the aforementioned analysis being conservative in nature. Further exploration of the unaccounted sources of RO_2 radicals will be presented in Section 4.3.

4. ***As mentioned by Referee #1 many more details on how the model simulations are performed are needed. In the manuscript it is mentioned that species listed in table S1 are used to set the boundary conditions for the base scenario. Which NMHC are included? From the kOH budget it appears a large variety of different VOC was measured. It would be good to list them. Is the precision, accuracy and limit of detection the same for all the different VOCs and OVOCs measured? Focusing on the kOH budget plot I would recommend separating the contribution of HCHO (which I assume now is included in the OVOC label) as I would guess it might be the largest fraction of the OVOCs.***

Reply:

Thank you for your reply. We have listed the VOCs involved in the model simulation in Table S3.

Table.S3. The comprehensive list of model constraints.

Categories	Species
Meteorology	Temperature, Relative humidity, Pressure, Jvalues
Trace gases	O_3, NO, NO_2, SO_2, CO, PAN, HONO
Alkanes	methane, ethane, propane, n-butane, isobutane, cyclopentane, n-pentane, isopentane, cyclohexane, methyl cyclopentane, 2,3-dimethyl butane,

	2,2-dimethyl butane, n-hexane, 2-methyl pentane, 3-methyl pentane, methyl cyclohexane, n-heptane, 2-methyl hexane, 2,3-dimethyl pentane, 2,4-dimethyl pentane, 3-methyl hexane, n-octane, 2,3,4-trimethyl pentane, 2-methyl heptane, 3-methyl heptane, 2,2,4-trimethyl pentane, n-nonane, n-decane, n-undecane, n-dodecane
Alkenes	ethene, propene, 1,3-butadiene, 1-butene, cis-2-butene, trans-2-butene, 1-pentene, cis-2-pentene, trans-2-pentene, 1-hexene, styrene
BVOCs	isoprene
Alkynes	acetylene
Aromatics	benzene, toluene,ethyl benzene, o-xylene, m-xylene, n-propyl benzene, isopropyl benzene, p-ethyl toluene, o-ethyl toluene, m-ethyl toluene, 1,2,4-trimethyl benzene, 1,3,5-trimethyl benzene, 1,2,3-trimethyl benzene, p-diethyl benzene, m-diethyl benzene
OVOCs	HCHO, acetaldehyde, MACR, MVK

The precision, accuracy, and detection limits for different VOCs and OVOCs measured using online GC-MS/FID are not the same, with some information on VOCs already listed in Table S2.

Table S2. Information table for parts of the VOC monitoring species by online GC-MS/FID. Revised by (Zhu et al., 2021).

Name	Molecular formula	m/z	MIR	Uncertainty	LOD
MTBE	$C_5H_{12}O$	88.15	0.73	3.3%	0.012
Ethane	C_2H_6	30.07	0.28	4.6%	0.013
Propane	C_3H_8	44.10	0.49	0.9%	0.010
n-Butane	C_4H_{10}	58.12	1.15	0.3%	0.012
Isobutane	C_4H_{10}	58.12	1.23	0.6%	0.008
Isopentane	C_5H_{12}	72.15	1.45	0.7%	0.008
n-Pentane	C_5H_{12}	72.15	1.31	1.5%	0.008
Cyclohexane	C_6H_{12}	84.16	1.25	1.5%	0.013
n-Hexane	C_6H_{14}	86.18	1.24	2.0%	0.006
2-Methylpentane	C_6H_{14}	86.18	1.5	3.8%	0.009
3-Methylpentane	C_6H_{14}	86.18	1.8	1.9%	0.009
Ethylene	C_2H_4	28.05	9	1.5%	0.013
Propene	C_3H_6	42.08	11.66	1.0%	0.010
Acetylene	C_2H_2	26.04	0.95	1.3%	0.018
Chloromethane	CH_3Cl	50.49	0.038	9.1%	0.011
Dichloromethane	CH_2Cl_2	84.93	0.041	3.2%	0.001
1,2-Dichloroethane	$C_2H_4Cl_2$	98.96	0.21	3.4%	0.001
1,2-Dichloropropane	$C_3H_6Cl_2$	112.99	0.29	1.1%	0.012
Chloroform	$CHCl_3$	119.38	0.022	1.2%	0.007
Freon-11	CCl_3F	137.40	/	4.6%	0.010
1,3-Dichlorobenzene	$C_6H_4Cl_2$	147.00	/	9.6%	0.022
Tetrachloromethane	CCl_4	153.82	0	1.5%	0.003
Freon-113	$C_2Cl_3F_3$	187.38	/	2.7%	0.004

Regarding the distribution of k_{OH}, the contribution of HCHO has been separately

identified according to the reviewers' opinions, and a more detailed discussion has been conducted on the contribution of OVOCs to OH reactivity (Fig. 4).

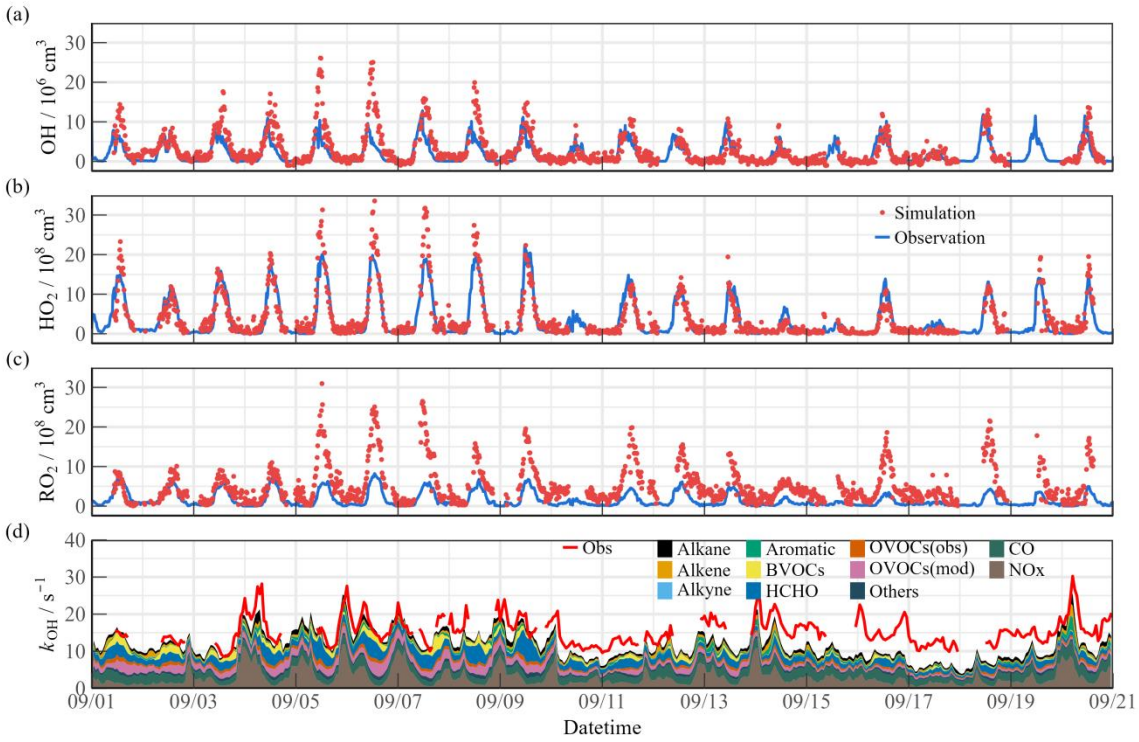

Fig. 4. Timeseries of the observed and modelled parameters for OH, HO_2 and k_{OH} during the observation period. **(a)** OH, **(b)** HO_2, **(c)** k_{OH}.

We added the description in Line 138-139&345-353&372-386.

Revision:

Line 139-140: Information table for parts of the VOC monitoring species by online GC-MS/FID was listed in Table S2.

Line 345-353: k_{OVOCs} are categorized into three groups: $k_{OVOCs(Obs)}$, $k_{OVOCs(Model)}$, and k_{HCHO}. Given the significance of formaldehyde photolysis, the contribution of HCHO to k_{OVOCs} is distinguished. $k_{OVOCs(Obs)}$ encompasses species observed in addition to formaldehyde, such as acetaldehyde (ACD) and the oxidation products of isoprene (MACR and MVK). Intermediates generated by the model, including glyoxal (GLY), methylglyoxal (MGLY), higher aldehydes (ALD), ketones (KET), methyl ethyl ketone (MEK), and methanol (MOH), are classified as $k_{OVOCs(Model)}$. Upon considering $k_{OVOCs(Model)}$, the reactivity calculated prior to September 10th aligns quite well with the observed OH reactivity.

Line 372-386: The calculated reactivity seems to compare well with the observed OH

reactivity at the start of the measurement period, but then there is evidence of missing OH reactivity after September 10th (Fig. 4(d)). Due to the limitations of available instruments, this observation only measured a limited number of OVOCs species, making it difficult to accurately quantify the contribution of larger aldehydes and ketones, carboxylic acids, nitrophenols, and other multifunctional species to k_{OH} (Wang et al., 2024). Since the MCM mechanism considers more secondary formation reactions than the RACM2 mechanism, it can qualitatively assess the photochemical role of unmeasured OVOCs species in the atmosphere (Wang et al., 2022b). The additional modeled OVOCs by the MCM v3.3.1 mechanism contributed ~2.4 s^{-1} to the missing OH reactivity (Fig. S7). During Heavy period, the reactivity of more model oxidation products increased the daytime k_{OH} by about 5.1 s^{-1}. Therefore, the observed k_{OH} can serve as an upper limit for sensitivity tests, thereby the full suite of radical measurement can be performed to explore the missing oxidation properties and ozone formation (Section 4.1).

5. It would be good to add the experimental budget for ROx as looking at table S1, all the species contributing substantially in the modelled budget (Fig 5) are measured. Or is Fig. 5 showing the experimental budget? And why did the author only analysis ROx and not OH, HO2 and RO2 separately?

Reply:

Thank you for your reply. We have added the experimental budget for OH, HO_2, RO_2 and the total ROx according to the reviewers' suggestions. We have newly added Section 2.4 which details the relevant methods for calculation, and have supplemented the experimental budget results in Fig. S8.

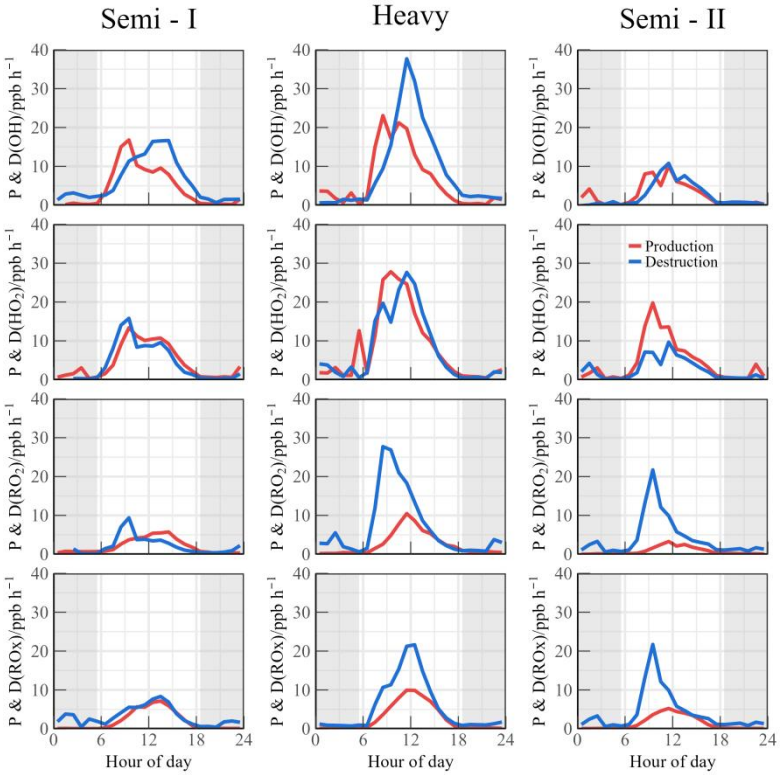

Fig. S8. Experimental budget for OH, HO_2, RO_2 and total ROx radicals during different periods.

Revision:

Line 269: 2.4 Experimental budget analysis

Line 270-284: In this study, an experimental radical budget analysis was also conducted (Eqs. (5) - (12)). Unlike model studies, this method relies solely on field measurements (concentrations and photolysis rates) and published chemical kinetic data, without depending on concentrations calculated by models(Whalley et al., 2021; Tan et al., 2019). Given the short-lived characteristics of OH, HO_2, and RO_2 radicals, it is expected that the concentrations are in a steady state, with total production and loss rates being balanced(Lu et al., 2019a). By comparing the known sources and sinks for radicals, unknown processes for initiation, transformation and termination can be determined.

$$P(OH) = j_{HONO}[HONO] + \varphi_{OH} j(O^1D)[O_3] + \Sigma i \left\{\varphi^i_{OH} k^i_{Alkenes+O_3}[Alkenes][O_3]\right\} + (k_{HO_2+NO}[NO] + k_{HO_2+O_3}[O_3])[HO_2] \quad (6)$$

$$D(OH) = [OH] \times k_{OH} \quad (7)$$

$$P(HO_2) = 2 \times j_{HCHO\_R}[HCHO] + \Sigma i\left\{\varphi^i_{HO_2} k^i_{Alkenes+O_3}[Alkenes][O_3]\right\} + (k_{HCHO+OH}[HCHO] + k_{CO+OH}[CO])[OH] + \alpha k_{RO_2+NO}[NO][RO_2] \quad (8)$$

$$D(HO_2) = (k_{HO_2+NO}[NO] + k_{HO_2+O_3}[O_3] + k_{HO_2+RO_2}[RO_2] + 2 \times k_{HO_2+HO_2}[HO_2])[HO_2] \quad (9)$$

$$P(RO_2) = \Sigma i\left\{\varphi^i_{RO_2} k^i_{Alkenes+O_3}[Alkenes][O_3]\right\} + k_{OH}[VOCs][OH] \quad (10)$$

$$D(RO_2) = \left\{(\alpha + \beta)k_{RO_2+NO}[NO] + (2 \times k_{RO_2+RO_2}[RO_2] + k_{HO_2+RO_2}[HO_2])\right\}[RO_2] \quad (11)$$

$$P(RO_x) = \Sigma i\left\{(\varphi^i_{OH} + \varphi^i_{HO_2} + \varphi^i_{RO_2}) k^i_{Alkenes+O_3}[Alkenes][O_3]\right\} + j_{HONO}[HONO] + \varphi_{OH} j(O^1D)[O_3] + 2 \times j_{HCHO\_R}[HCHO] \quad (12)$$

$$D(RO_x) = (k_{OH+NO_2}[NO_2] + k_{OH+NO}[NO])[OH] + \beta k_{RO_2+NO}[NO] + 2 \times (k_{RO_2+RO_2}[RO_2][RO_2] + k_{HO_2+RO_2}[HO_2][RO_2] + k_{HO_2+HO_2}[HO_2][HO_2]) \quad (13)$$

In which, j(HONO), j(O^1D) are the measured photolysis rates of HONO and O_3, respectively, and jHCHO_R is the measured photolysis rate for the channel of formaldehyde photolysis generating HO_2. φ_{OH} represent the OH yield in the O_3 photolysis reaction. φ^i_{OH}, $\varphi^i_{HO_2}$ and $\varphi^i_{RO_2}$ are the yields for the ozonolysis reaction producing OH, HO_2, and RO_2, respectively. α is the proportion of RO_2 radicals reacting with NO that are converted to HO_2, and β is the proportion of alkyl nitrates formation, which are set to 1 and 0.05, respectively(Tan et al., 2019).

Line 407-433: By comparing the known sources and sinks for radicals, unknown processes for initiation, transformation and termination can be determined in the experimental budget analysis (Fig. S8). During the Semi I period, the production and destruction rates of HO_2, RO_2, and total ROx radicals were very consistent, but a significant lack of a source term for OH radicals was existed after 10:00. This missing source became more pronounced during the Heavy period, reaching 16 ppb/h at noon,

which is close to the results observed by AIRPRO, but three times that observed by Heshan in PRD region(Tan et al., 2019; Whalley et al., 2021). The ratio of OH production-to-destruction rate during the Semi II period was close to 1, indicating consistency between the observed results of OH, HO_2, k_{OH}, and other precursors(Whalley et al., 2018). However, the generation of HO_2 radicals in the morning was about twice as high as the removal rate, suggesting that there are contributions from unconsidered HO_2 radical removal channels (such as heterogeneous reactions)(Song et al., 2021). During the Heavy period, there was a rapid total removal rate of RO_2 radicals, reflecting the dominated HO_2 generation by the reaction of RO_2 radicals with NO. Although the P(HO_2) and D(HO_2) were quite in balance, the removal rate of RO_2 radicals far exceeded the known production rate (especially before 12:00). Previous work has shown that halogen chemistry (such as photolysis of nitryl chloride ($ClNO_2$)) could be an important source in the morning time, but this was not included in the calculation of ROx or RO_2 budget in this campaign. The steady-state analysis for HO_2 radical in the London campaign emphasized that only by significantly reducing the observed RO_2-to-HO_2 propagation rate to just 15% could balance both P(HO_2) and D(HO_2), indicating that the RO_2-related mechanism for propagation to other radical species may not be fully understood(Whalley et al., 2018). Therefore, based on the current knowledge seems unlikely to explain the required source-sink difference of nearly 25 ppb/h in the RO_2 budget. Sensitivity analysis is needed to further infer the causes of the difference for the experimental budget analysis.

6. ***Co-authors of this study just recently published a new mechanisms that could explain the missing OH source at low NO (Yang et al., 2024). This could be a good sensitivity test rather than species X and I would recommend the authors to try it.***

Reply:

Thank you for your review and valuable comments on this manuscript. We agree with your perspective on species X, considering that it currently serves more as a

fitting parameter, which may offer limited assistance in understanding the underlying mechanisms. Therefore, in this revision, we have followed your advice and added the Higher Aldehyde Mechanism to test whether it can explain the discrepancy between measured and simulated radical concentrations. The results indicate that the contribution of the HAM mechanism to OH radicals in different episodes ranged between 4.4% - 6.0%, while the concentrations of HO_2 and RO_2 radicals increased by approximately 7.4% and 12.5%, respectively.

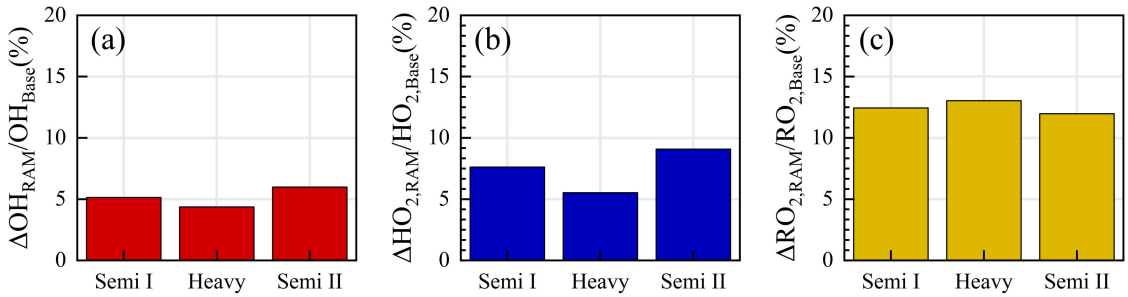

Fig. 7. The response of **(a)** OH, **(b)** HO_2 and **(c)** RO_2 radicals to the Higher Aldehyde Mechanism (HAM) in different episodes (Semi I, Heavy, and Semi II) in diurnal time (10:00-15:00).

Additionally, we combine the missing aldehyde primary emissions and the HAM mechanism under the entire photochemical spectrum to qualitatively assess the impact on RO_2 radical concentrations. Notably, RO_2 radical concentrations exhibit a pronounced sensitivity to autoxidation, with the incorporation of additional OVOCs potentially boosting simulated RO_2 radical concentrations by 20% to 40%. Consequently, although limiting formaldehyde can partially offset the HO_2 radical cycle and enhance the precision of HOx radical chemistry studies, additional measurements should be undertaken for other OVOCs, coupled with the deployment of full-chain radical detection systems, to accurately elucidate the oxidation processes under severe ozone pollution conditions.

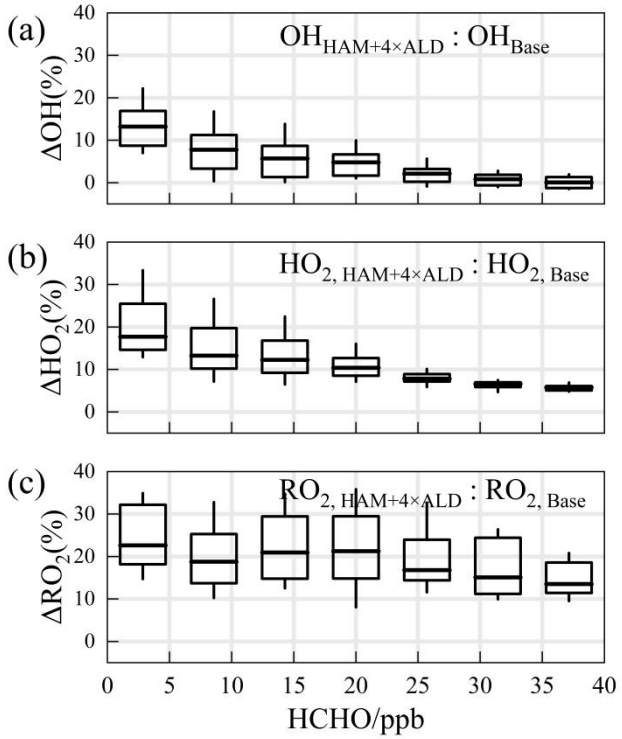

Fig. S12. The relationship between the differences in the simulation of **(a)** OH, **(b)** HO_2, and **(c)** RO_2 radical concentrations by HAM mechanism and the base scenario across the entire photochemical spectrum. An empirical hypothesis is proposed to amplify the concentration of higher-order aldehydes by a factor of about 4, which is the proportion of formaldehyde concentration underestimated by the model. The boxplots represent the 10%, 25%, median, 75%, and 90% of the data, respectively.

Revision:

Line 508-518: Missing OH sources are closely related to the chemistry of OVOCs(Yang et al., 2024a; Qu et al., 2021). Reactive aldehyde chemistry, particularly the autoxidation of carbonyl organic peroxy radicals ($R(CO)O_2$) derived from higher aldehydes, is a significant OH regeneration mechanism that has been shown to contribute importantly to OH sources in regions with abundant natural and anthropogenic emissions during warm seasons(Yang et al., 2024b). In this study, the higher aldehyde mechanism (HAM) by Yang et al was parameterized into the base model to test new insights into the potential missing radical chemistry (Fig. 7). The results indicate that the contribution of the HAM mechanism to OH radicals in different episodes ranged between 4.4% - 6.0%, while the concentrations of HO_2 and RO_2 radicals increased by approximately 7.4% and 12.5%, respectively.

Line 556-569: Higher aldehyde chemistry is a concrete manifestation of verifying the aforementioned hypothesis for RO_2 sources(Yang et al., 2024b). The autoxidation

process of $R(CO)O_2$, encompasses a hydrogen migration process that transforms it into the ·OOR(CO)OOH radical(Wang et al., 2019). This radical subsequently reacts with NO to yield the ·OR(CO)OOH radical. The ·OR(CO)OOH radical predominantly undergoes two successive rapid hydrogen migration reactionss, ultimately resulting in the formation of HO_2 radicals and hydroperoxy carbonyl (HPC). Consequently, the HAM mechanism extends the lifetime of the RO_2 radical, providing a valuable complement to the unaccounted sources of RO_2 radicals. As depicted in Fig. 7, the incorporation of the HAM mechanism results in an approximate 7.4% and 12.5% increase in the concentrations of HO_2 and RO_2 radicals, respectively. It is important to note that the total concentrations of primary emitted aldehydes and the HPC group may be underestimated, which could lead to the aforementioned analysis being conservative in nature. Further exploration of the unaccounted sources of RO_2 radicals will be presented in Section 4.3.

Line 682-712: The reasons for the discrepancy between simulated and observed values for ozone production deserve further investigation. As depicted in Fig.11(c), the simulated HO_2/RO_2 ratios display a robust positive correlation with photochemical activity, fluctuating between 2 and 4. A notable feature during severe ozone pollution is the intense distribution of formaldehyde, with an average concentration of 21.81 ± 4.57 ppb (11:00 – 13:00). While formaldehyde acts as a precursor for HO_2 radicals, it does not directly generate RO_2 radicals. The contributions of OVOCs to the ROx radical do not exhibit the same intensity as formaldehyde, and the current mechanism encounters difficulties in replicating formaldehyde concentrations (Fig. S11). The simulation of formaldehyde concentrations using the MCM v3.3.1 mechanism has shown improvement, indicating that the secondary formation of unmeasured species, such as OVOCs, will feedback on RO_2 radical levels. When formaldehyde levels are unconstrained, the simulated HO_2/RO_2 ratios align with observations, suggesting that under the prevailing chemical mechanism, the photochemical efficiency of formaldehyde and other OVOCs is similar. Therefore, an empirical hypothesis is proposed to amplify the concentration of higher-order aldehydes by a factor of about 4, which is the proportion of formaldehyde concentration underestimated by the model.

The qualitative assessment of the impact of missing aldehyde primary emissions on RO_2 radical concentrations was combined with the HAM mechanism across the entire photochemical spectrum (Fig.S12). Enhanced impact of aldehyde autoxidation in the presence of weak photochemical conditions could alter the simulated levels of OH and HO_2 radicals by approximately 13.9% and 18.1%, respectively. However, higher ALD concentrations will be achieved under intensive photochemical conditions, leading to the gradual dominance of the sink channels for OH + OVOCs, with the effect of autoxidation mechanisms gradually decreasing. RO_2 radical concentrations is notably more sensitive to the HAM mechanism, where incorporates additional OVOCs, can enhance the simulation of RO_2 radical concentrations by 20 - 40%. Consequently, although limiting formaldehyde can partially offset the HO_2 radical cycle and enhance the precision of HOx radical chemistry studies, additional measurements should be undertaken for other OVOCs, coupled with the deployment of full-chain radical detection systems, to accurately elucidate the oxidation processes under severe ozone pollution conditions.

Minor Comments

1. *“ The full-chain radical detection untangled a gap-bridge between the photochemistry and the intensive oxidation level in the chemical-complex atmosphere, enabling a deeper understanding of the tropospheric radical chemistry at play.” (Page 2, Lines 42-45)*

Reply:

Thank you for your suggestion, the abstract section has been re-optimized.

Revision:

Line 30-48: At a heavy ozone pollution episode, the oxidation capacity reached an intensive level compared with other sites, and the simulated OH, HO_2, and RO_2 radicals provided by the RACM2-LIM1 mechanism failed to adequately match the observed data both in radical concentration and experimental budget analysis. Sensitivity tests utilizing a comprehensive set of radical measurements revealed that the higher aldehyde mechanism (HAM) effectively complements the non-traditional regeneration of OH radicals, yielding enhancements of 4.4% - 6.0% compared to the base scenario, while the concentrations of HO_2 and RO_2 radicals have shown increments of about 7.4% and 12.5%, respectively. Notably, RO_2 radical concentrations exhibit a pronounced sensitivity to autoxidation, with the incorporation of additional OVOCs potentially boosting simulated RO_2 radical concentrations by 20% to 40%. The incorporation of larger alkoxy radicals stemming from monoterpenes has refined the consistency between measurements and modeling in the context of ozone production under elevated NO levels, diminishing the disparity from 4.17 to 2.33. This outcome corroborates the hypothesis of sensitivity analysis as it pertains to ozone formation. Moving forward, by implementing a comprehensive radical detection approach, further investigations should concentrate on a broader range of OVOCs to rectify the imbalance associated with RO_2 radicals, thereby providing a more precise understanding of oxidation processes during severe ozone pollution episodes.

2. *“Moreover, the closure experiment, incorporating field campaigns and box*

model, has proven to be an effective method for verifying the integrity of radical chemistry at local to global scales.” (Page 3, Lines 70-72). I do not know what the closure experiment is?

Reply:

Thank you for your reply, we have revised the relevant description in Line 73-75.

Revision:

Line 73-75: Moreover, the union of comprehensive field campaigns and box model, has proven to be an effective method for verifying the integrity of radical chemistry at local to global scales (Lu et al., 2019b; Tan et al., 2018).

References

Färber, M., Fuchs, H., Bohn, B., Carlsson, P. T. M., Gkatzelis, G. I., Marcillo Lara, A. C., Rohrer, F., Vereecken, L., Wedel, S., Wahner, A., and Novelli, A.: Effect of the Alkoxy Radical Chemistry on the Ozone Formation from Anthropogenic Organic Compounds Investigated in Chamber Experiments, ACS ES&T Air, 1, 1096-1111, 10.1021/acsestair.4c00064, 2024.

Lu, K., Guo, S., Tan, Z., Wang, H., Shang, D., Liu, Y., Li, X., Wu, Z., Hu, M., and Zhang, Y.: Exploring atmospheric free-radical chemistry in China: the self-cleansing capacity and the formation of secondary air pollution, Natl. Sci. Rev., 6, 579-594, 10.1093/nsr/nwy073, 2019a.

Lu, K. D., Guo, S., Tan, Z. F., Wang, H. C., Shang, D. J., Liu, Y. H., Li, X., Wu, Z. J., Hu, M., and Zhang, Y. H.: Exploring atmospheric free-radical chemistry in China: the self-cleansing capacity and the formation of secondary air pollution, Natl. Sci. Rev., 6, 579-594, 10.1093/nsr/nwy073, 2019b.

Ma, X., Tan, Z., Lu, K., Yang, X., Chen, X., Wang, H., Chen, S., Fang, X., Li, S., Li, X., Liu, J., Liu, Y., Lou, S., Qiu, W., Wang, H., Zeng, L., and Zhang, Y.: OH and HO_2 radical chemistry at a suburban site during the EXPLORE-YRD campaign in 2018, Atmos Chem Phys, 22, 7005-7028, 10.5194/acp-22-7005-2022, 2022.

Qu, H., Wang, Y., Zhang, R., Liu, X., Huey, L. G., Sjostedt, S., Zeng, L., Lu, K., Wu, Y., Shao, M., Hu, M., Tan, Z., Fuchs, H., Broch, S., Wahner, A., Zhu, T., and Zhang, Y.: Chemical Production of Oxygenated Volatile Organic Compounds Strongly Enhances Boundary-Layer Oxidation Chemistry and Ozone Production, Environ Sci Technol, 10.1021/acs.est.1c04489, 2021.

Song, H., Lu, K., Dong, H., Tan, Z., Chen, S., Zeng, L., and Zhang, Y.: Reduced Aerosol Uptake of Hydroperoxyl Radical May Increase the Sensitivity of Ozone Production to Volatile Organic Compounds, Environmental Science & Technology Letters, 9, 22-29, 10.1021/acs.estlett.1c00893, 2021.

Tan, Z. F., Lu, K. D., Dong, H. B., Hu, M., Li, X., Liu, Y. H., Lu, S. H., Shao, M., Su, R., Wang, H. C., Wu, Y. S., Wahner, A., and Zhang, Y. H.: Explicit diagnosis of the local ozone production rate and the ozone-NOx-VOC sensitivities, Sci. Bull., 63, 1067-1076, 10.1016/j.scib.2018.07.001, 2018.

Tan, Z. F., Lu, K. D., Hofzumahaus, A., Fuchs, H., Bohn, B., Holland, F., Liu, Y. H., Rohrer, F., Shao, M., Sun, K., Wu, Y. S., Zeng, L. M., Zhang, Y. S., Zou, Q., Kiendler-Scharr, A., Wahner, A., and Zhang, Y. H.: Experimental budgets of OH, HO_2, and RO_2 radicals and implications for ozone formation in the Pearl River Delta in China 2014, Atmos Chem Phys, 19, 7129-7150, 10.5194/acp-19-7129-2019, 2019.

Wang, H., Ma, X., Tan, Z., Wang, H., Chen, X., Chen, S., Gao, Y., Liu, Y., Liu, Y., Yang, X., Yuan, B., Zeng, L., Huang, C., Lu, K., and Zhang, Y.: Anthropogenic monoterpenes aggravating ozone pollution, Natl. Sci. Rev., 9, 2022a.

Wang, S.-n., Wu, R.-r., and Wang, L.-m.: Role of Hydrogen Migrations in Carbonyl Peroxy Radicals in the Atmosphere, Chinese J Chem Phys, 32, 457-466, 10.1063/1674-0068/cjcp1811265, 2019.

Wang, W., Yuan, B., Su, H., Cheng, Y., Qi, J., Wang, S., Song, W., Wang, X., Xue, C., Ma, C., Bao, F., Wang, H., Lou, S., and Shao, M.: A large role of missing volatile organic compound reactivity from anthropogenic emissions in ozone pollution regulation, Atmos Chem Phys, 24, 4017-4027, 10.5194/acp-24-4017-2024, 2024.

Wang, W., Yuan, B., Peng, Y., Su, H., Cheng, Y., Yang, S., Wu, C., Qi, J., Bao, F., Huangfu, Y., Wang, C., Ye, C., Wang, Z., Wang, B., Wang, X., Song, W., Hu, W., Cheng, P., Zhu, M., Zheng, J., and Shao, M.: Direct observations indicate photodegradable oxygenated volatile organic compounds (OVOCs) as

larger contributors to radicals and ozone production in the atmosphere, Atmos Chem Phys, 22, 4117-4128, 10.5194/acp-22-4117-2022, 2022b.
Whalley, L. K., Stone, D., Dunmore, R., Hamilton, J., Hopkins, J. R., Lee, J. D., Lewis, A. C., Williams, P., Kleffmann, J., Laufs, S., Woodward-Massey, R., and Heard, D. E.: Understanding in situ ozone production in the summertime through radical observations and modelling studies during the Clean air for London project (ClearfLo), Atmos Chem Phys, 18, 2547-2571, 10.5194/acp-18-2547-2018, 2018.
Whalley, L. K., Slater, E. J., Woodward-Massey, R., Ye, C., Lee, J. D., Squires, F., Hopkins, J. R., Dunmore, R. E., Shaw, M., Hamilton, J. F., Lewis, A. C., Mehra, A., Worrall, S. D., Bacak, A., Bannan, T. J., Coe, H., Percival, C. J., Ouyang, B., Jones, R. L., Crilley, L. R., Kramer, L. J., Bloss, W. J., Vu, T., Kotthaus, S., Grimmond, S., Sun, Y., Xu, W., Yue, S., Ren, L., Acton, W. J. F., Hewitt, C. N., Wang, X., Fu, P., and Heard, D. E.: Evaluating the sensitivity of radical chemistry and ozone formation to ambient VOCs and NOx in Beijing, Atmos Chem Phys, 21, 2125-2147, 10.5194/acp-21-2125-2021, 2021.
Woodward-Massey, R., Sommariva, R., Whalley, L. K., Cryer, D. R., Ingham, T., Bloss, W. J., Ball, S. M., Cox, S., Lee, J. D., Reed, C. P., Crilley, L. R., Kramer, L. J., Bandy, B. J., Forster, G. L., Reeves, C. E., Monks, P. S., and Heard, D. E.: Radical chemistry and ozone production at a UK coastal receptor site, Atmos Chem Phys, 23, 14393-14424, 10.5194/acp-23-14393-2023, 2023.
Yang, X., Li, Y., Ma, X., Tan, Z., Lu, K., and Zhang, Y.: Unclassical Radical Generation Mechanisms in the Troposphere: A Review, Environ Sci Technol, 10.1021/acs.est.4c00742, 2024a.
Yang, X., Wang, H., Lu, K., Ma, X., Tan, Z., Long, B., Chen, X., Li, C., Zhai, T., Li, Y., Qu, K., Xia, Y., Zhang, Y., Li, X., Chen, S., Dong, H., Zeng, L., and Zhang, Y.: Reactive aldehyde chemistry explains the missing source of hydroxyl radicals, Nat Commun, 15, 1648, 10.1038/s41467-024-45885-w, 2024b.
Zhu, B., Huang, X.-F., Xia, S.-Y., Lin, L.-L., Cheng, Y., and He, L.-Y.: Biomass-burning emissions could significantly enhance the atmospheric oxidizing capacity in continental air pollution, Environ. Pollut., 285, 10.1016/j.envpol.2021.117523, 2021.